脇谷先生とACE-IT ・・それから

第１幕

と　き　：1985年～1987年
ところ　：核融合科学研究所
キャスト：脇谷一義とACE-ITメンバー

はじめに

- 背景
  - ・多価イオンの電離断面積

    直接電離過程、
    励起－自動電離過程、共鳴捕獲－２重自動電離過程

- ACE-ITの目的
  - ・電子分光法を用いた（多価）イオンの励起過程

    散乱電子のエネルギー損失スペクトル
    放出電子のエネルギースペクトル

Giessen

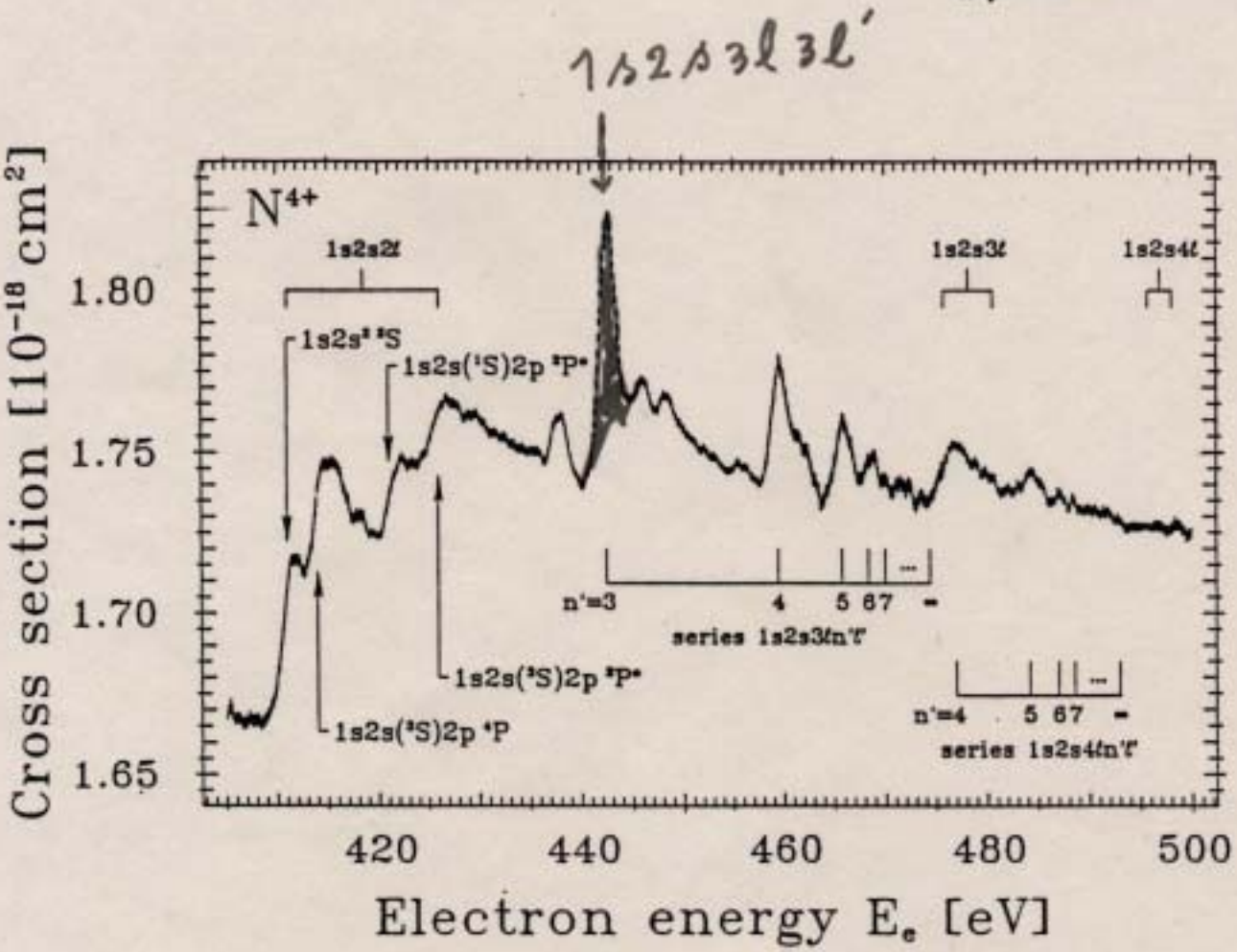

Figure 11. Cross sections for indirect contributions to electron impact ionization of Li-like N^{4+} ions[38]. The scan data were smoothed over bins of seven adjacent points of the original measurement. Assignments of states to the observed features are given on the basis of calculations using the code of Grant et al.[39]. Two series of Rydberg states involving $\Delta n = 2$ and $\Delta n = 3$ transitions can be recognized: 1s2s3lnl' (n = 3,4,5,6...) and 1s2s4lnl' (n = 4,5,...). The series limits 1s2s3l and 1s2s4l are at the thresholds for direct inner-shell excitations. The ranges of corresponding energy levels[47] are indicated.

The new measurements reveal even more structure than might have been expected simply on the basis of the model calculation[33] for a Na-like ion shown in Fig. 9. Apparently there are other resonance series and steps and dips in the cross section which make it difficult to see a clear excitation-autoionization feature. The resonance contributions (the snow) appear to be much higher than the excitation steps (the stairs) on top of which they are observed. One particular series of resonances between 51 eV and 55 eV is interpreted to be due to $2p^5 3s3pnl$ configurations; i. e. the Rydberg series corresponding to the one in Fig. 9. Peaks up to n = 6 are resolved, the higher Rydberg states lump together due to the limited energy resolution of the experiment. An upper limit of 0.3 eV to the energy spread is set by the width of the resonance observed at 55.5 eV. The strongest REDA peak observed makes up for about 3.5 % of the total ionization cross section at that particular energy. By this measurement a first experimental step is made towards the old challenge to see REDA processes in sodium-like Fe^{15+} ions.

Strong REDA resonances have also been found in the ionization of lithium-like ions[37,38] B^{2+}, C^{3+}, N^{4+}, O^{5+} and F^{6+}. A scan measurement on N^{4+} is shown in Fig. 11. Details in the vicinity of the excitation-autoionization threshold were studied (see also Fig. 7). Individual terms of the 1s2s2l excited configurations are resolved. In addition many resonance features are found.

W

Ba+

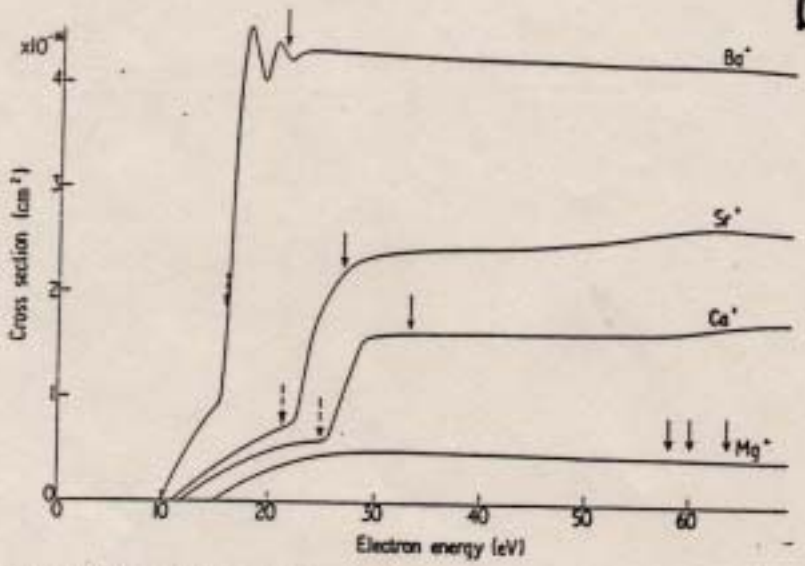

Figure 1. Observed ionization functions for the ground states of Ba^+, Sr^+, Ca^+ and Mg^+. The experimental results for Sr^+ and Ca^+ are from Peart and Dolder (1975), also the figure is taken from their paper, while the results for Ba^+ and Mg^+ are from Peart *et al* (1973) and Martin *et al* (1968), respectively. For Ba^+, Sr^+ and Ca^+, the calculated $(p^5d\ ^3P)s\ ^2P$ (broken arrows) and $(^1P)^2P$ (arrows) thresholds are indicated. For Mg^+, the $2p^5(3p^2\ ^1D)^2P$, $2p^5(3d3s\ ^3D)^2P$ and $2p^5(3d3s\ ^1D)^2P$ thresholds, in order of increasing energy, are shown. The $2p^5(3p^2\ ^1D)^2P$ and $2p^5(3d3s\ ^1D)^2P$ terms are strongly mixed as explained in the text.

Ba+ 5p-5d

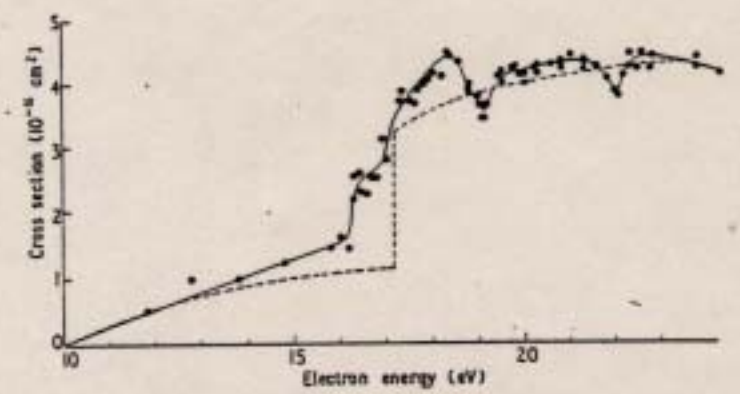

Figure 1. Cross sections for the ionization of Ba^+ plotted against incident electron energy. Autoionization thresholds are resolved at energies of 15·8, 16·8, 19·2 and 21·9 eV. – – – results of calculations by Bely *et al* (1971).

拡がりは約2.9eVである。両ビームはチョッピングされており、両方のビームが出ているときの真空は、1×10^{-9}Torr以下に保たれている。

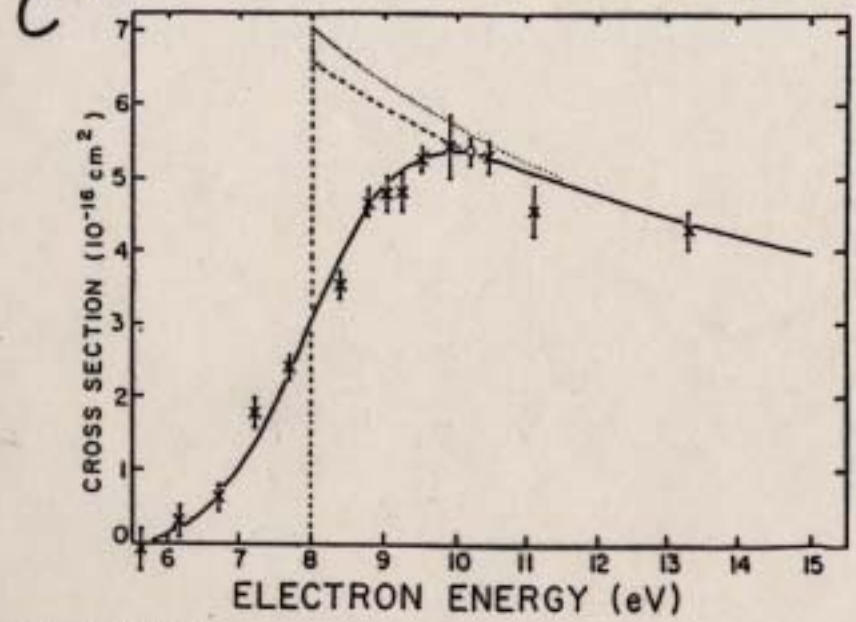

Fig. II - 3 - 5. Cross section vs electron energy for $e + C^{3+}(2\,^2S_{1/2}) \rightarrow e + C^{3+}(2\,^2P_{1/2,3/2})$. Open circle is an absolute measurement. Crosses are measured relative to the open circle. The dashed curve: two-state close-coupling (Ref. 10). Dotted curve: unitarized Coulomb-Born with exchange (Ref. 10). Solid curve: "expected" cross section (see text) resulting from convolution of electron energy distribution with the two-state close-coupling calculation. Bars represent statistical uncertainties at 90% confidence level. There are additional systematic uncertainties totaling ± 17% at "good confidence level" (see text).

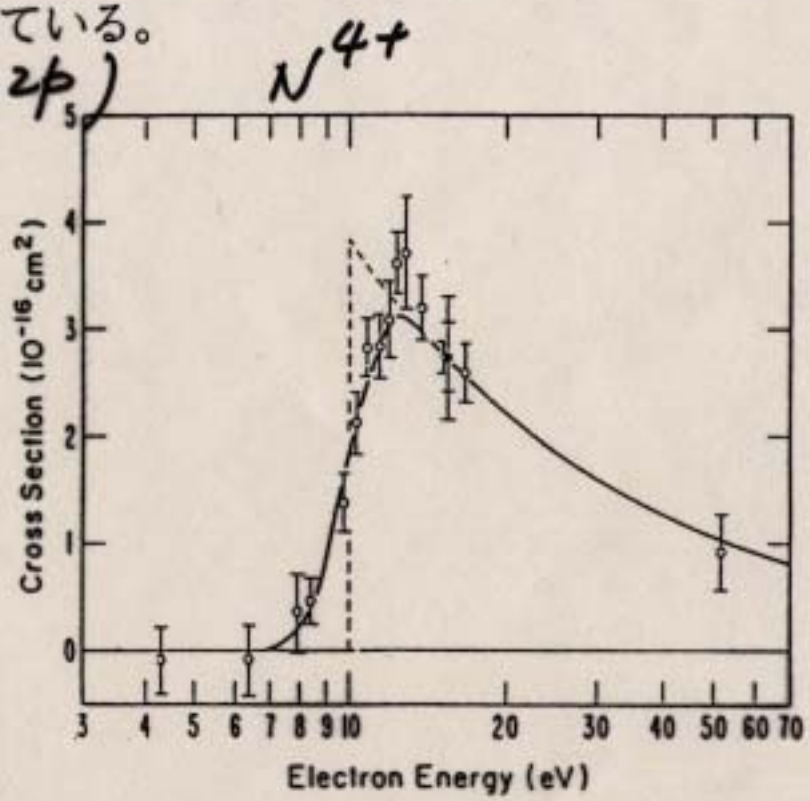

Fig. II - 3 - 6. Absolute cross section vs electron energy for $2s-2p$ excitation of N^{4+} by electron impact. Solid point at 15.5 eV represents an absolute measurement, relative to which open points at other energies were measured. Dashed curve represents two-state close coupling with exchange calculation (2CCX) from Ref. 19, and solid curve is a convolution of the experimental electron energy distribution with the dashed curve. Bars on experimental points designate random uncertainties at 90% confidence level, and outer bars on solid point represent the total experimental uncertainty at good confidence level (see Table I and text).

Zn^+ (4S−4P)

$Zn^+(4s\ ^2S\text{-}4p\ ^2P,\ 4s\ ^2S\text{-}3d^94s^2\ ^2D)$[12,13,14]

JPLのグループから３つの実験結果が
断面積の測定は一連の実験の中で最初
最初の実験は、電子の散乱角度を（
30,40,50,60,75,85,100eVと変えてZn⁺(²S
ルギー損失スペクトルが測られた[13]。
す。スペクトロメーターの総合分解能
ない。また、残留ガスとの非弾性散乱
る。得られたエネルギー損失スペクト
その強度から次のようにして励起の微
1）フォームファクターFは電子ビー
幅は計算機シミュレーションによる
2）立体角ΔΩ、透過率T、検出効率η
ら推定された。透過率と検出効率の
て得られた微分断面積をTable 1.に示
その後の実験でFの値が入射電子のエ
今回の実験で得られた微分断面積のエ
る。

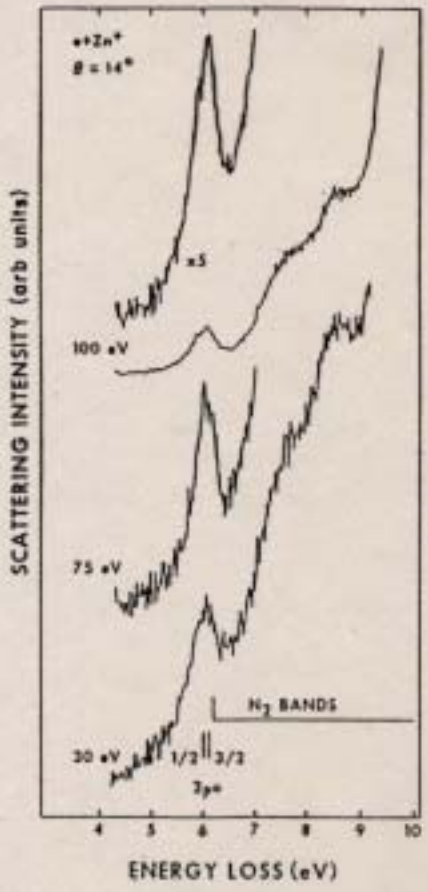

Fig. III – 14. Experimental energy-loss spectra of the $^2S_{1/2} - {}^2P_{1/2,3/2}$ resonance transition in Zn II at $\theta = 14°$ scattering angle, 6-keV ion energy, and at the indicated electron energies. Energy-loss transitions in molecular N_2 are responsible for the rising background. The onset of these transitions [the (0,0) band of the $X - A$ Vegard-Kaplan system] is shown.

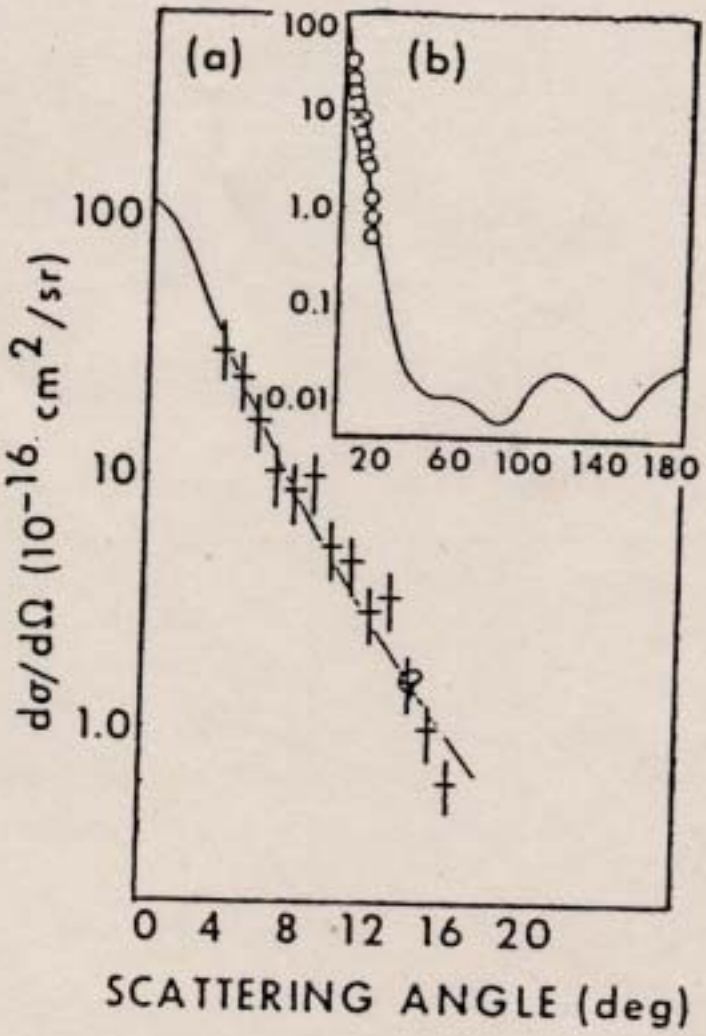

Table 1. Relative and absolute differential cross sections for excitation of the resonance transition $^2S_{1/2} - {}^2P_{1/2,3/2}$ in Zn II at $\theta = 14°$.

Electron energy (eV)	Relative cross section	Absolute cross section (10^{-17} cm²/sr)*
30	1.32 ± 0.24	4.63
40	1.89 ± 0.34	6.63
	1.46 ± 0.26	5.13
50	2.53 ± 0.40	8.88
60	2.83 ± 0.31	9.93
75	3.69 ± 0.37	13.0
85	2.58 ± 0.21	9.05
100	1.00 ± 0.13	3.51

*With an error estimate of 33⅓%.

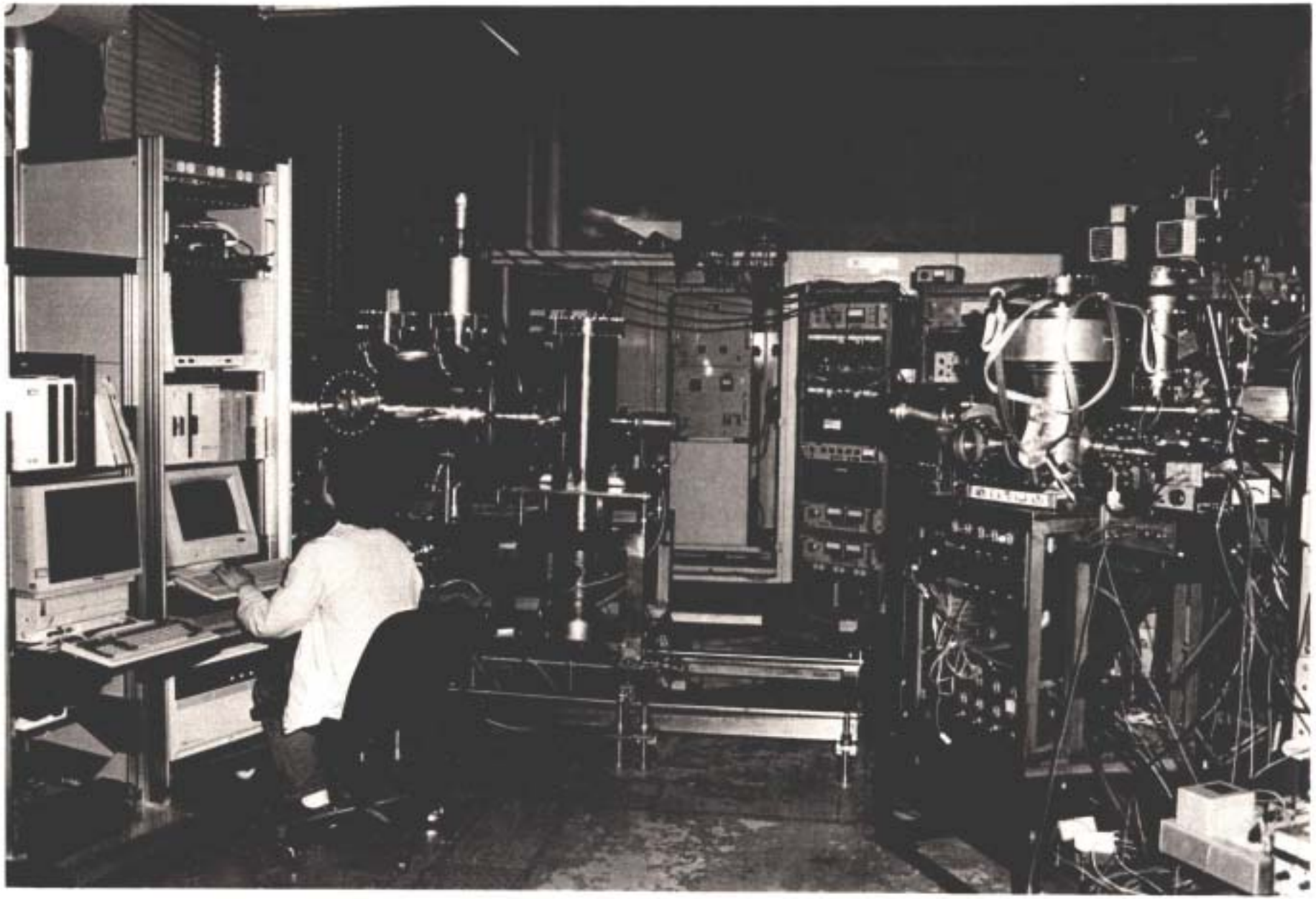

1985. 8. 24日(土)

- TMP + チェンバーベーク = 5×10^{-7} torr
- チェンバーベーク中止して2時後 DV の Main あける
- TMP + DV = 9×10^{-8} torr

1) SAS に高電圧加える。バックグランドが目でみてチカチカ光ることをたしかめる。

2) He 1×10^{-6} torr
elastic のビーム通らず。Pre-Amp は高温 80°C のため中に入れられない。

本日はここで中止。

ビール・ウイスキーかるく飲んでから

「へのへのへもじ」にゆく。

1985. 8. 25(日)

1) コントロールパネルの配線にミスあり。PER がフィラメントセンターに接触していたので正しく配線する。

2) elastic めでたくキャチ出来た。

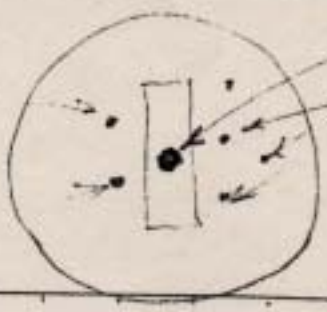

今夜は「風ろいぼー」にゆく

1985.8.27日(火)

高エネルギー研究所発表会,

No.

檀上氏用データをとること

Date

を目的に頑張ることにする。

- 真空度 TMP+DP+クライオ(48°K きのうより悪い)=3.0×10^{-8} Torr
- He を 9.0×10^{-7} torr 入れる
- MCPの表面の位置がAnalyserの集束面上にあるか調べたがなかなかむずかしい。3本のベローのネジを正しく平行に移動させなくてはならない。結果あまり変化なし。現在ベローの長さ27.5mmで最短になっている。すなわち一番深く入りこんでいる。

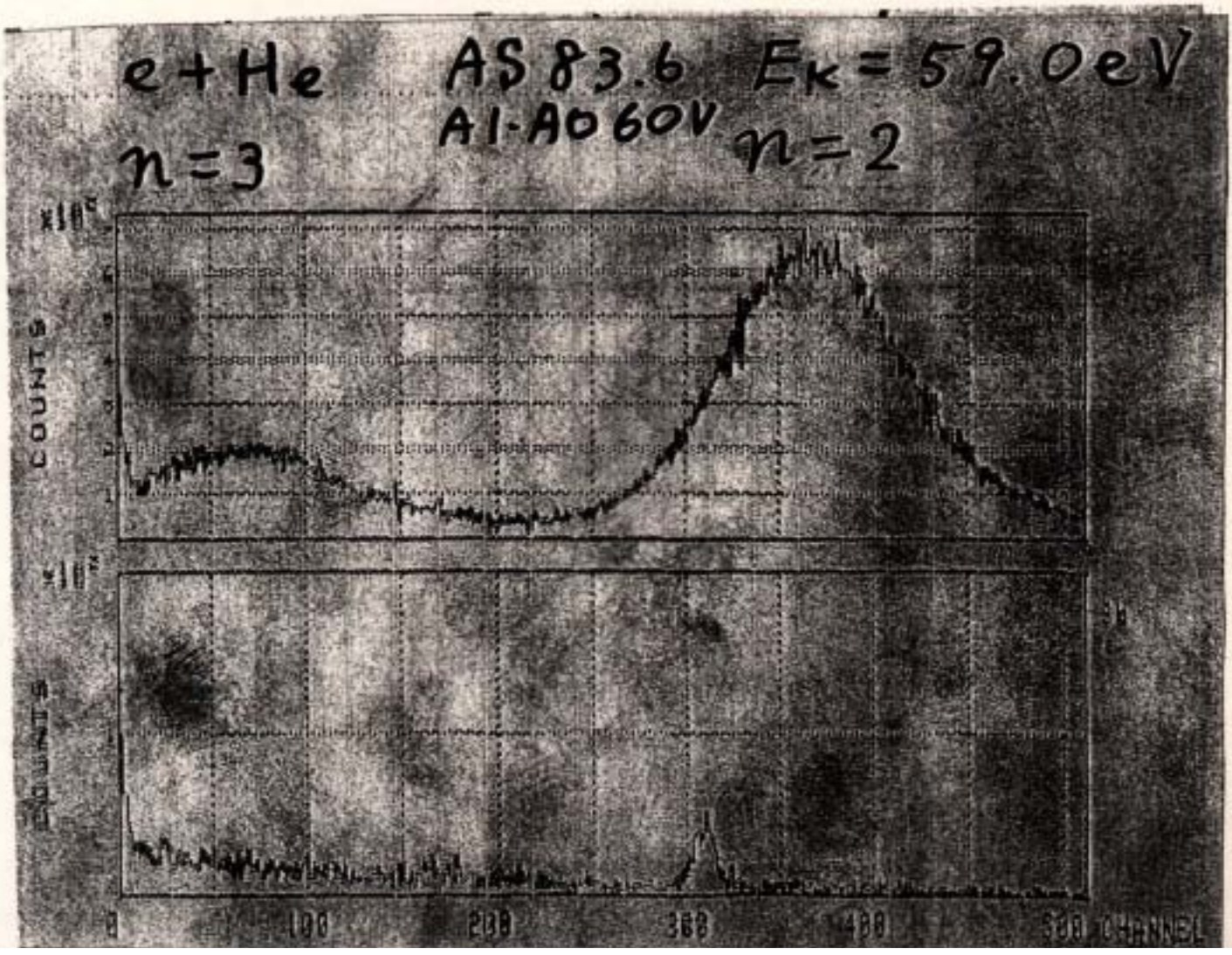

１９８５年忘年会
年明けて１９８６年

ハロゲンランプの破裂事故

３／７～３／１４

真空容器内のよごれ

６／２８

いろいろありまして、はや６月

e + Ba^+

10/30

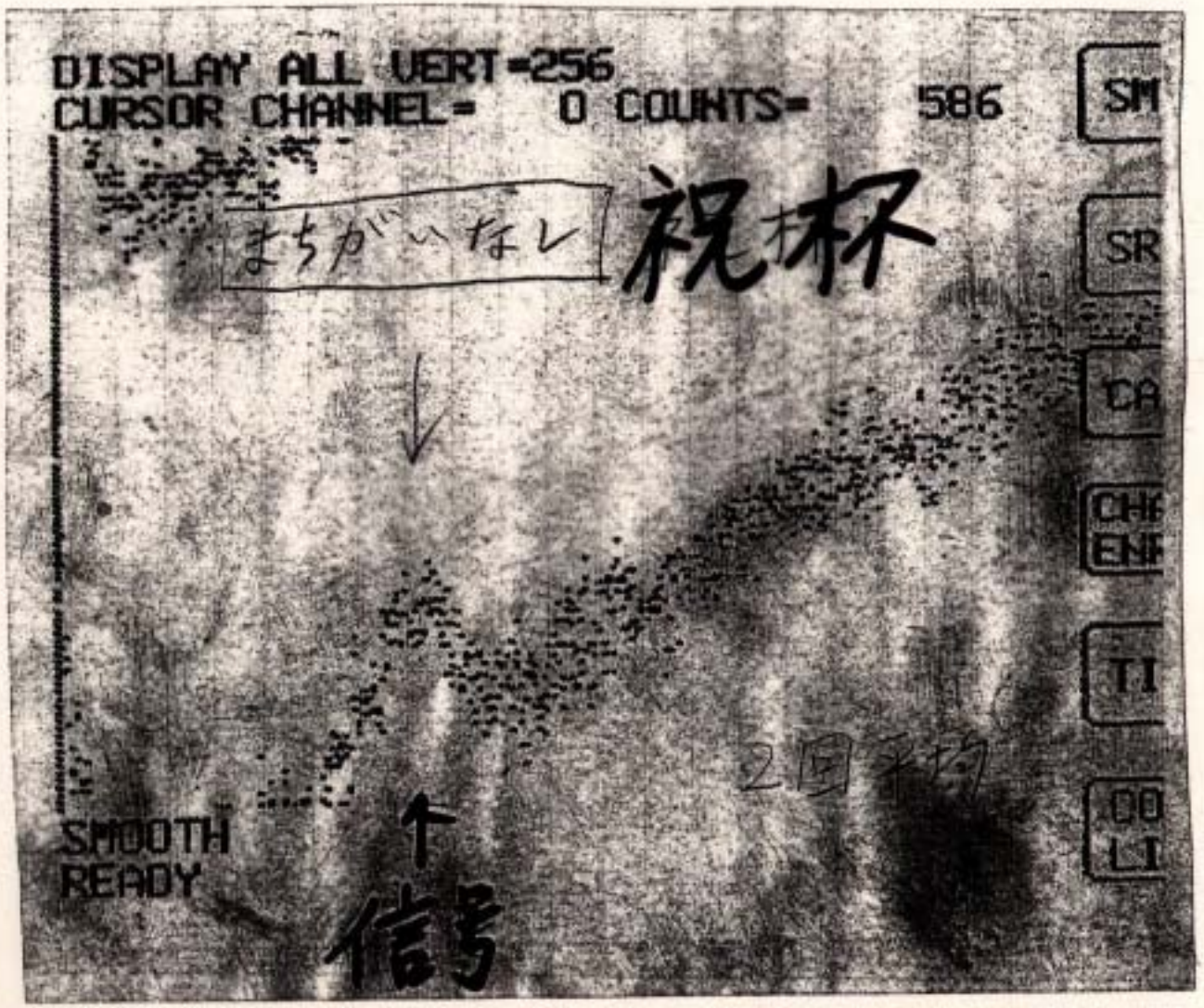

50回
蓄積

600V
10°

Ba^+ ナヨッピングなし。

なんと美しい

12月11日

大谷 様

忘年会は中止してデータが出てから盛大にしませんか。
12月23日もし忘年会するとしたら遠方でなく名大の方が小生は都合がよいのですが。23日は慶応が終ってからゆけば8時半ごろつきます。24日以後は冬休みとなりますので日程はいつでも何です。忘年会よりもデータを出す方が気分がよいのですが。

上京のさいには「千恵」さんにゆきましょう。

明けて１９８７年

$E_e = 50\,eV$

新しい場所に何か出てきた

$E_e = 60\,eV$ でも出た。

~9.5 eV

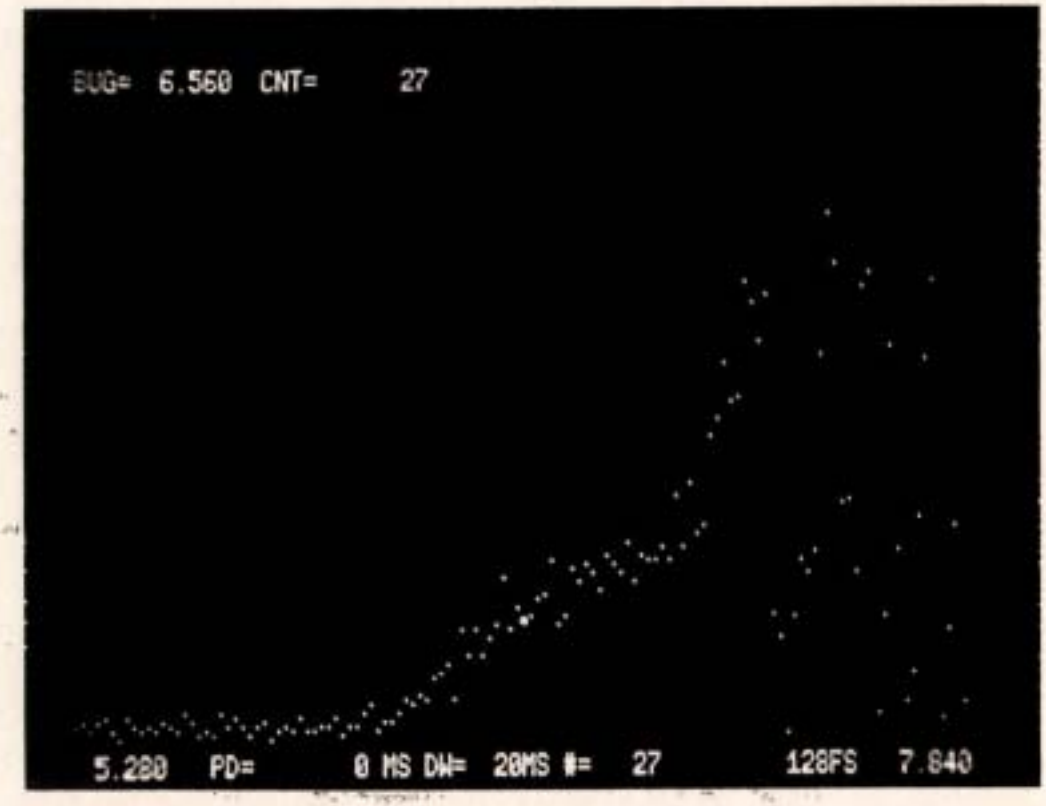

⑥ ⑦

9.5 eV

high energy electron impact 外キ (>50eV

１０月３１日（金）

- 電子衝突エネルギーが下がるとCross Sectionが大きくなるのでE_K=10eVまで下げた。

  E_K=10eVではノイズが多くてあきらめた。

  E_K=２０eVにしてテスト。

  うまくゆかず。

以上　脇谷談

以後　女神は現れず

それから

第２幕

重点領域研究「多価イオン原子物理学」

多価イオンと物質との相互作用

放出電子スペクトル法による多価イオンの多電子励起状態の研究

多価イオン－電子衝突による励起過程の研究

と　き：１９９３年～

ところ：上智大学、東京都立大学

A. Huber et al
RL 67, 1407('91) $e + Ar^{7+}$ 3s−3p

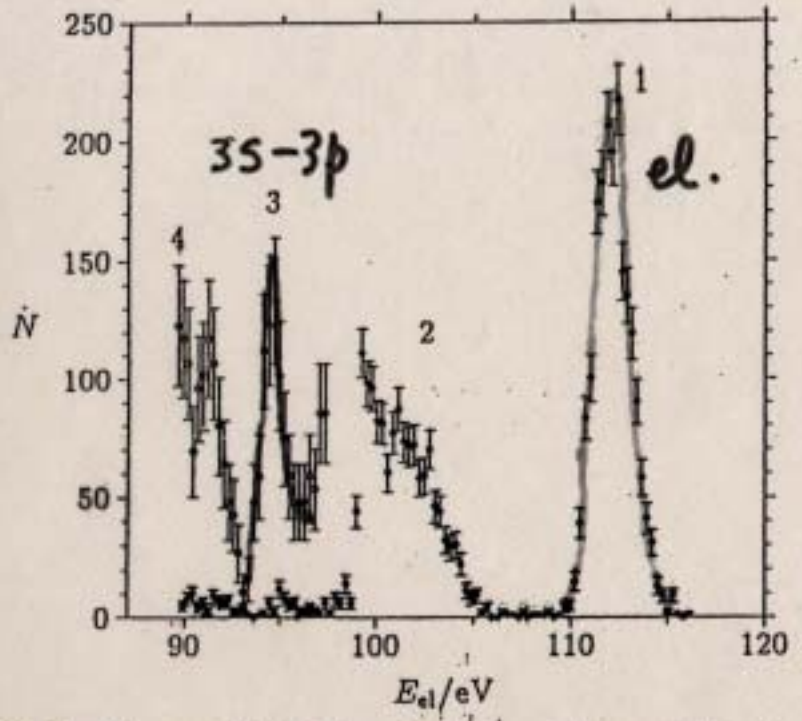

FIG. 1. Energy distribution of electrons being scattered at an angle of 24° by Ar^{7+} ions and by the background gas. Primary electron energy: 100 eV. 1, Elastic electron-ion signal; 2, elastic scattering by the residual gas; 3, signal due to the $3s$-$3p$ excitation; 4, inelastic electron–residual-gas scattering.

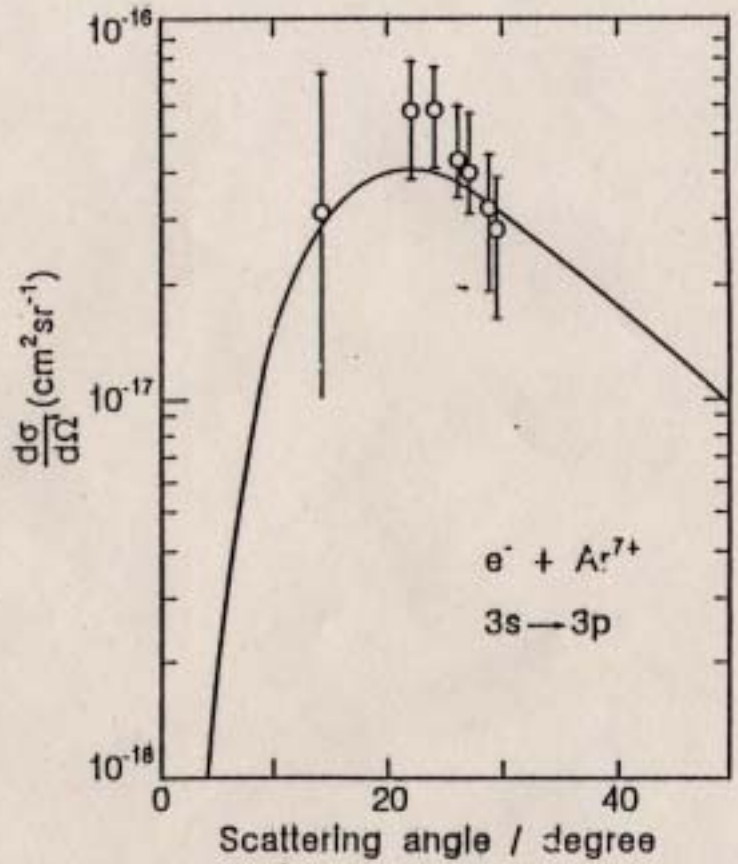

FIG. 4. Angular differential excitation cross section for the resonant $3s$-$3p$ transition in Ar^{7+}. Electron energy: 100 eV. Experiment: open circles; theory: solid curve.

$e + Ar^{7+}$ (3s−3p)；宮崎大，宇宙研

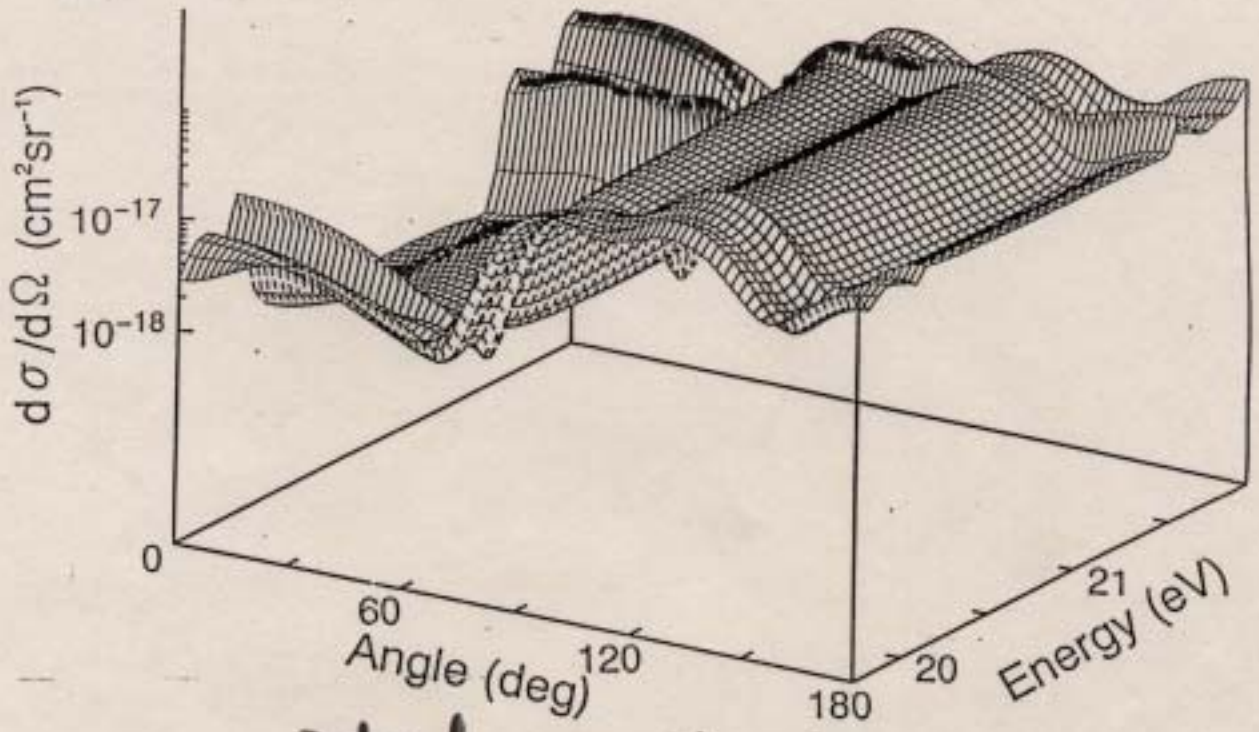

$3s + e \rightarrow 3d\,n\ell \quad 4\ell' n\ell \rightarrow 3p + e$

$E_{ex} = 17.4\,eV$

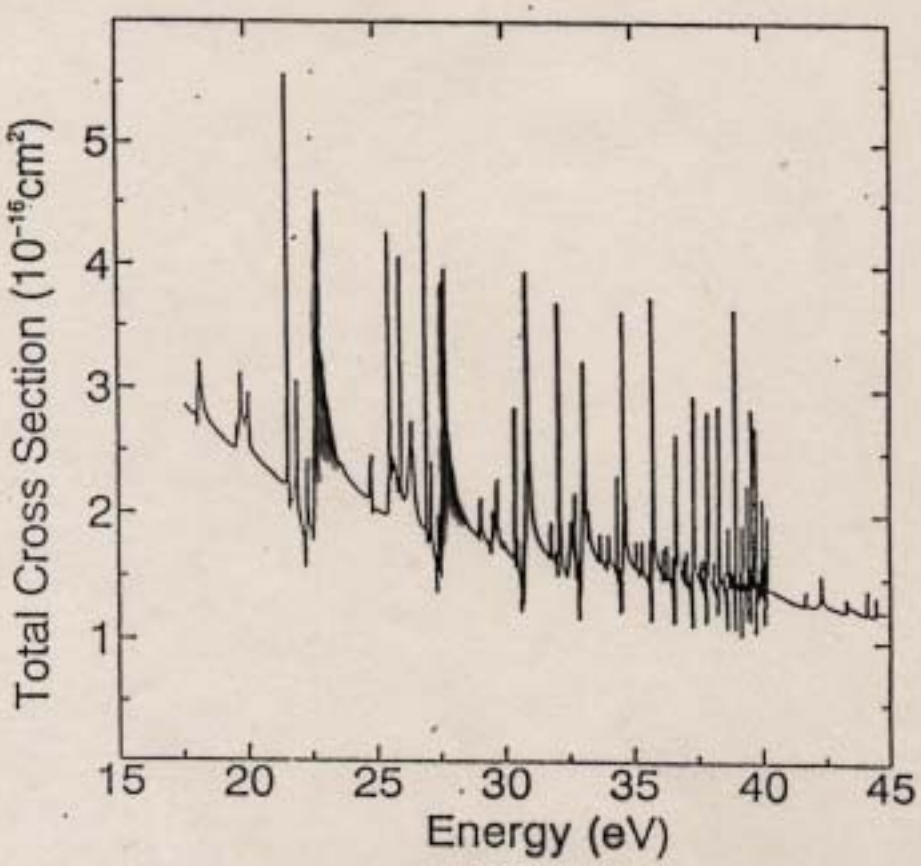

図1. Ar^{7+} の3s−3p遷移におけるR−行列法の積分断面積

S. Nakazaki et al

Toroidal analyzer

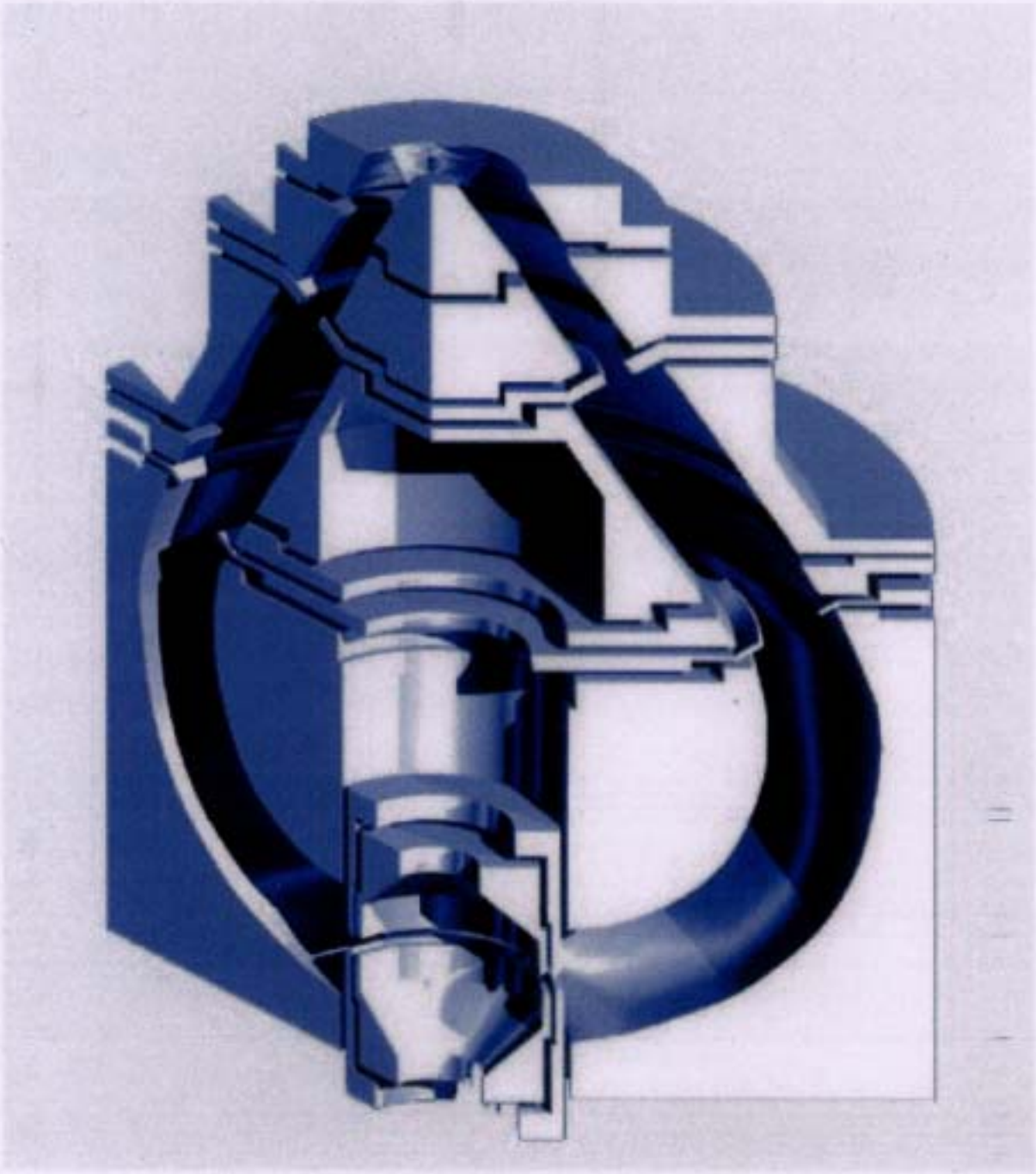

It consists of a pair of toroidal deflectors and lenses.
Entrance slit is 1 mm wide and circularly extended.

Conditions

✓**Residual gas pressure**

Base pressure	$< 1 \times 10^{-10}$ Torr
Both beams ON	1.4×10^{-10} Torr

✓**Ion beam** (Ar^{q+}, q = 7, 8)

Energy	15 × q keV
Current	1.5 μA
Diameter (FWHM)	0.5 mmϕ

✓**Electron beam**

Energy	80.0 eV (Ar^{7+}), 78.6 eV (Ar^{8+})
Current	1.5 μA
Diameter (FWHM)	0.5 mmϕ

✓**Collision energy (CM)** **100 eV**

✓**Toroidal analyzer**

Pass energy (E_{pass})	100 eV (small angle)
	110 eV (large angle)
Angular range	30° - 120°
Energy range	$0.9E_{pass}$ -$1.1E_{pass}$
Relative energy resolution	1 %

xperimental setup

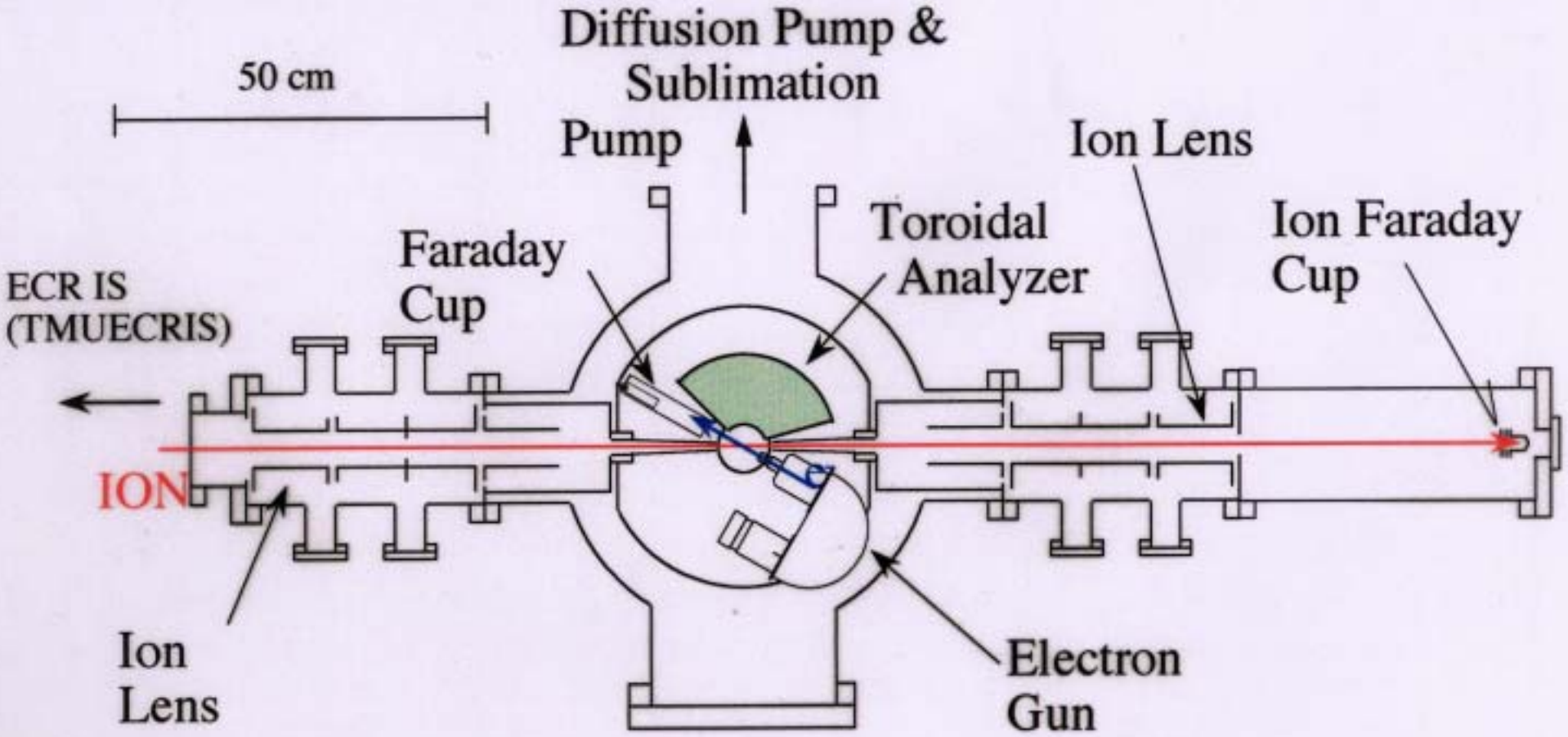

Ions are extracted from 14.25 GHz electron cycrotron resonance (ECR) ion source, and are mass analyzed and focused at the collision center.

Electron scattering from HOPG

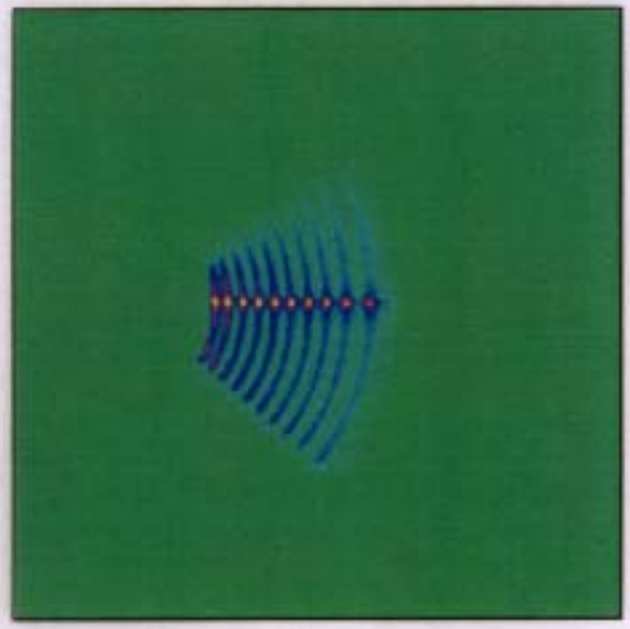

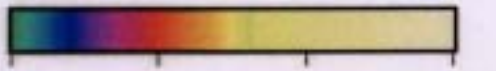

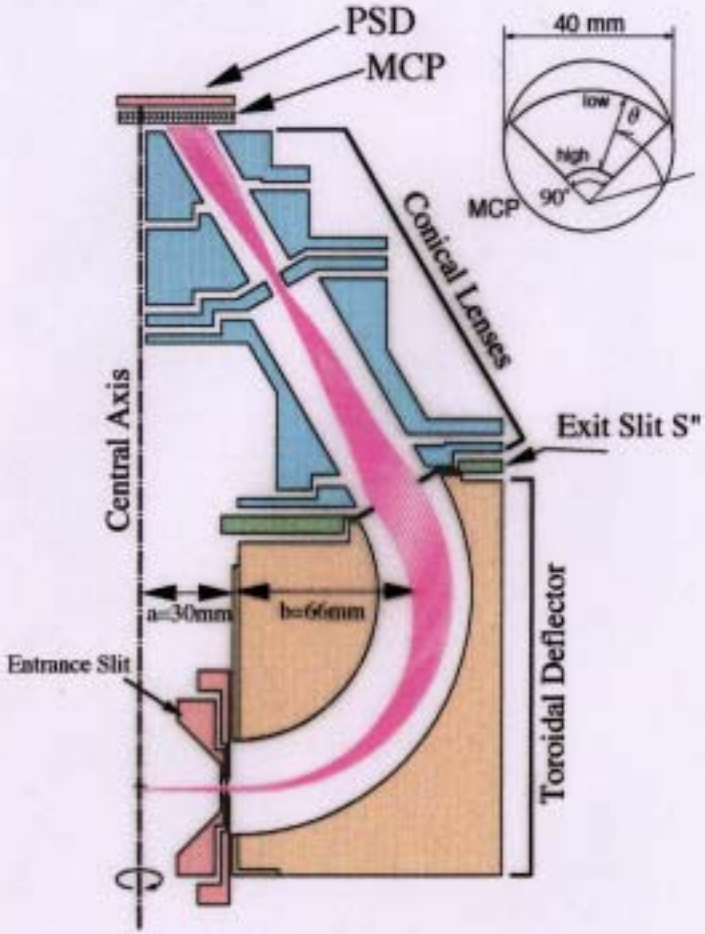

Electron images on the two dimensional detector. Images are on the concentric circles and its center is the image point of the collision center. Innermost image is for the electrons with energy of 110 eV and outermost image is for 92 eV electrons. Bright spots are from the electrons scattered at mirror reflection angle, in the present case 75^0 with respect to the incident electron direction.

Detection efficiency

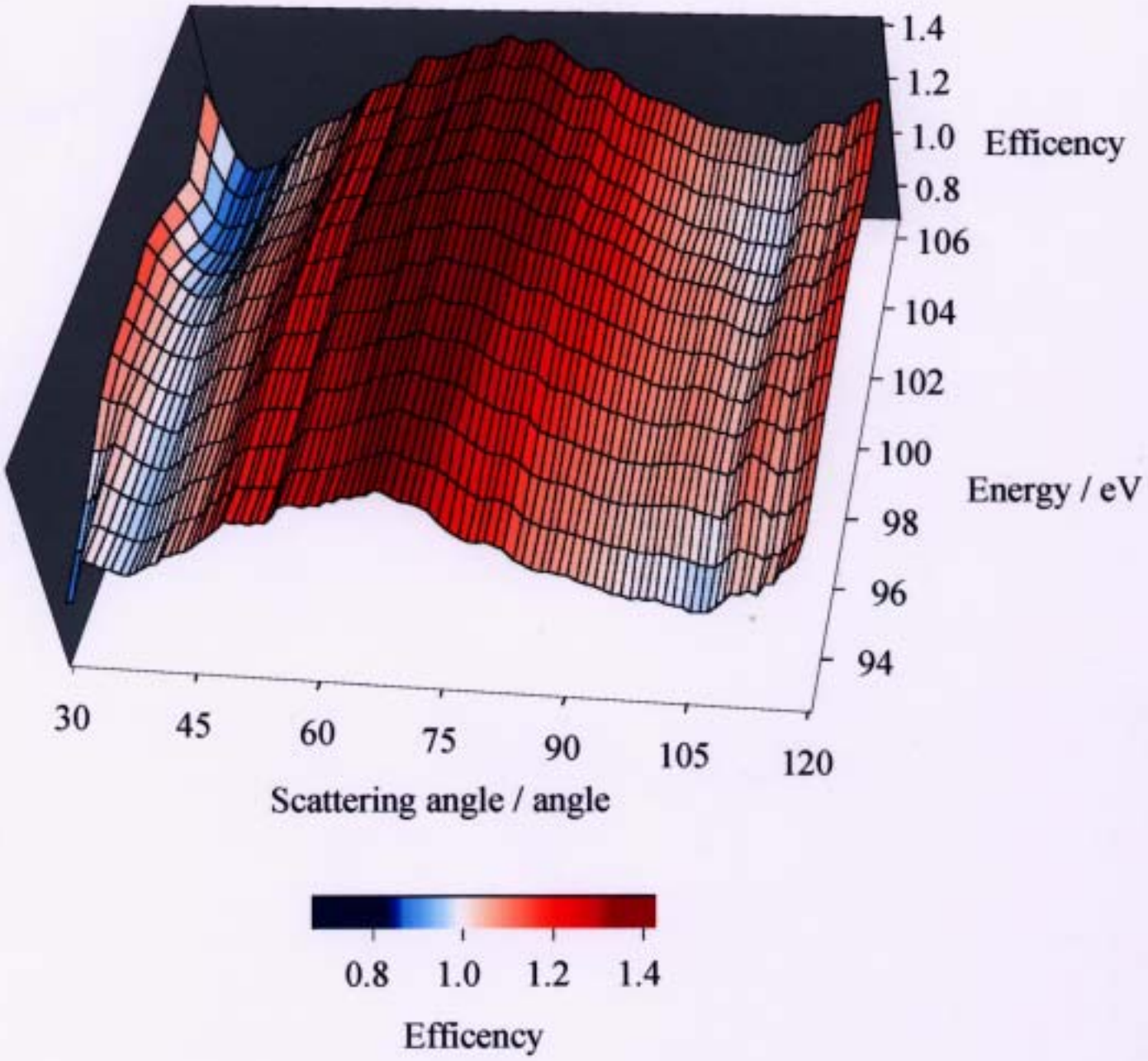

Raw data

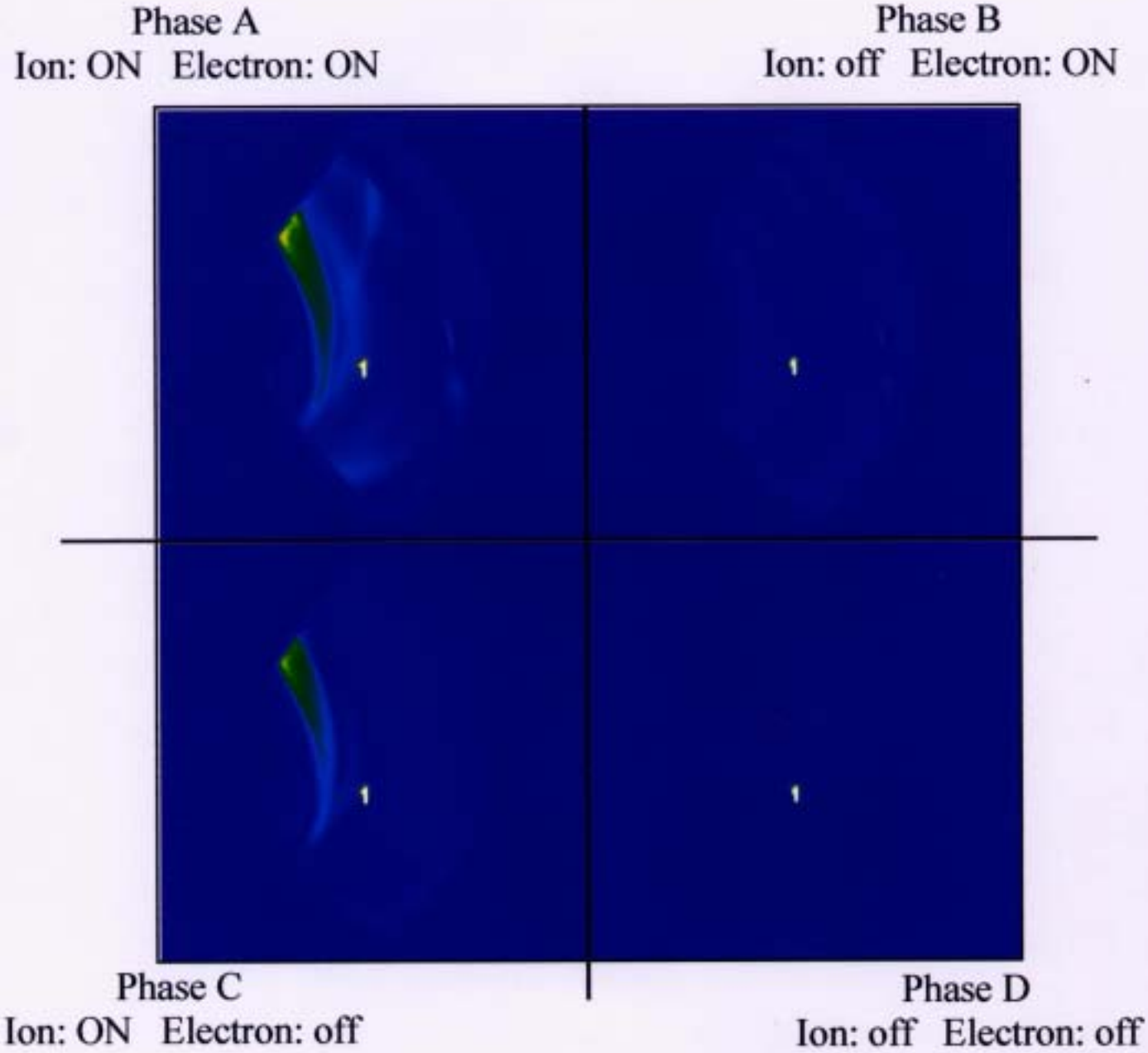

Raw data in the double beam chopping experiment.

Subtracted image

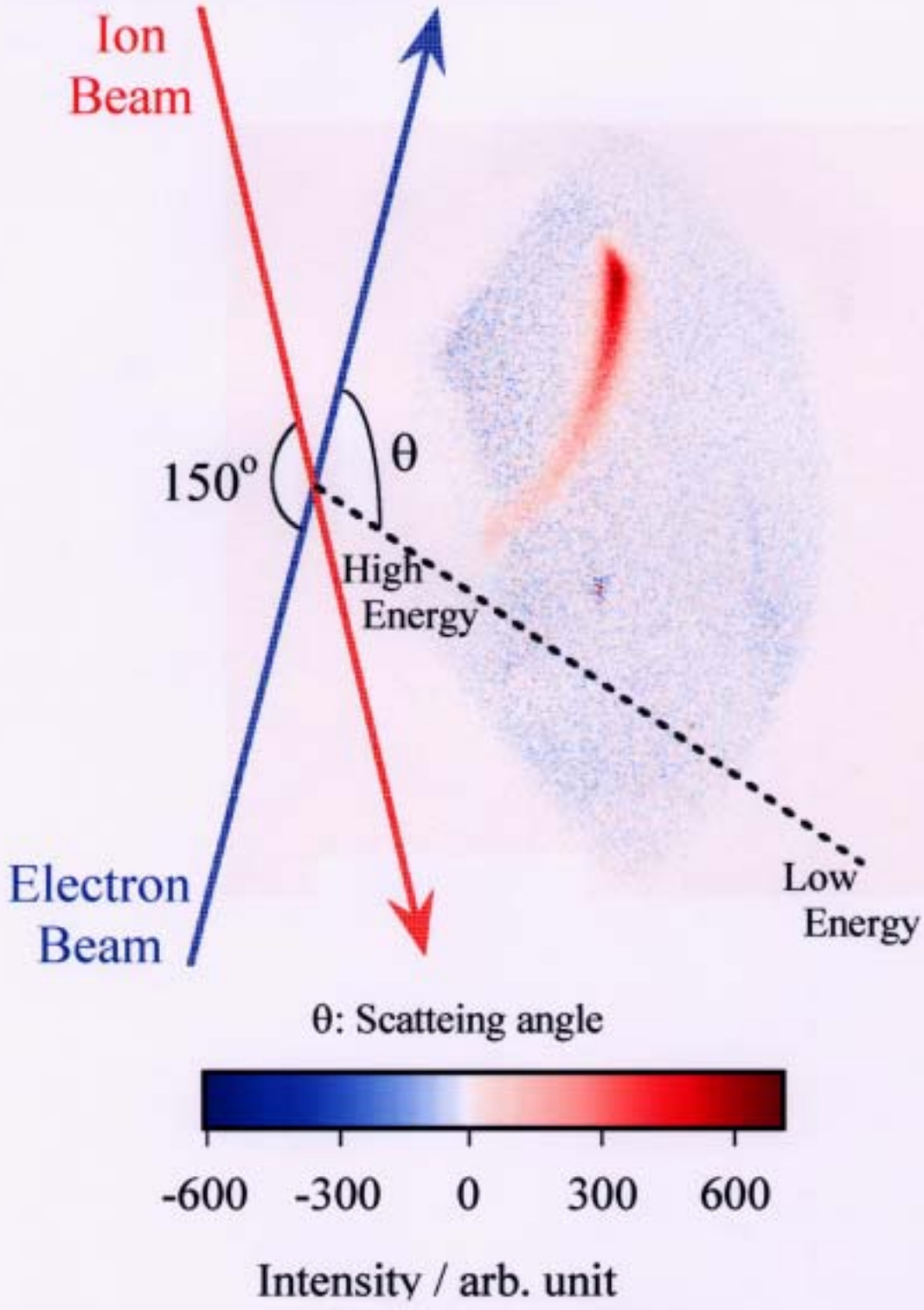

Two dimensional electron image for elastic scattering from Ar^{7+} ions at the collision energy of 100 eV.

Relative DCS (e^- - Ar^{7+})

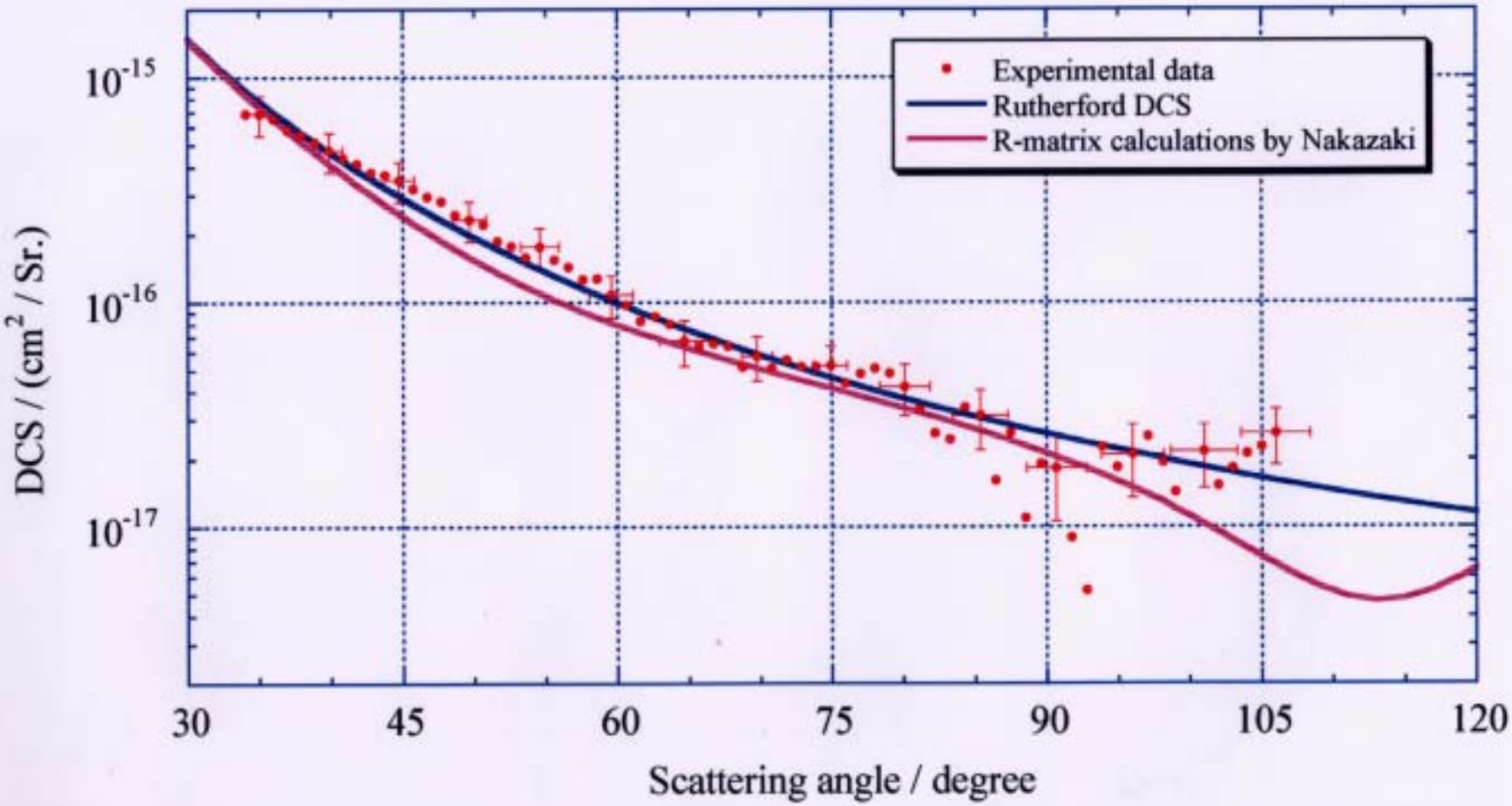

Fig. Normalized cross sections for elastic scattering of electrons from Ar^{7+} ions at E_{CM} = 100 eV.
Red dots : Experimental data. Blue line : Rutherford cross sections.
Purple line : R-matrix calculations by Nakazaki.
Error bars are ploted at the 1σ confidence level.

Relative DCS (e^- - Ar^{8+})

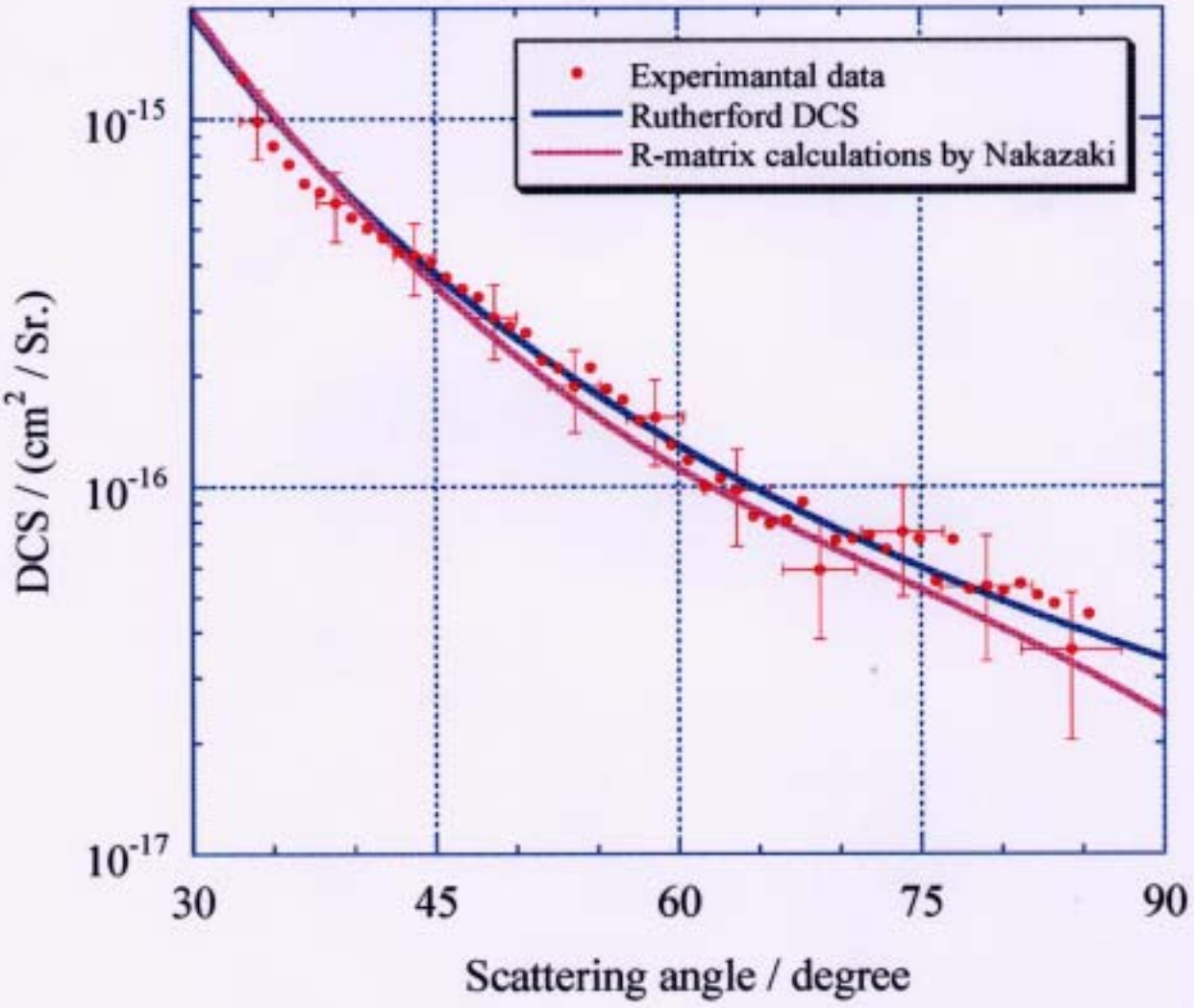

Fig. Normalized cross sections for elastic scattering of electrons from Ar^{8+} ions at E_{CM} = 100 eV.

Red dots : Experimental data.

Blue line : Rutherford cross sections.

Purple line : R-matrix calculations by Nakazaki.